PAPER

Large, weakly basic bis(carboranyl)phosphines: an experimental and computational study†‡

Laura E. Riley,[a] Tobias Krämer, [iD] *[a] Claire L. McMullin,[b] David Ellis,[a] Georgina M. Rosair,[a] Igor B. Sivaev[c] and Alan J. Welch [iD] *[a]

The bis(carboranyl)phosphines [μ-2,2′-PPh-{1-(1′-1′,2′-*closo*-C$_2$B$_{10}$H$_{10}$)-1,2-*closo*-C$_2$B$_{10}$H$_{10}$}] (**I**) and [μ-2,2′-PEt-{1-(1′-1′,2′-*closo*-C$_2$B$_{10}$H$_{10}$)-1,2-*closo*-C$_2$B$_{10}$H$_{10}$}] (**1**) have been prepared and spectroscopically and structurally characterised. Crystallographic and DFT computational studies of **1** suggest that the orientation of the ethyl group, relative to the bis(carborane), is the result of intramolecular dihydrogen bonding. This orientation is such that the magnitudes of the $^2J_{PH}$ coupling constants are approximately equal but of opposite sign, and fast exchange between the methylene protons in solution leads to an observed $^2J_{PH}$ close to zero. The steric properties of **I**, **1** and their derivatives [μ-2,2′-P(Ph)AuCl-{1-(1′-1′,2′-*closo*-C$_2$B$_{10}$H$_{10}$)-1,2-*closo*-C$_2$B$_{10}$H$_{10}$}] (**2**) and [μ-2,2′-P(Et)AuCl-{1-(1′-1′,2′-*closo*-C$_2$B$_{10}$H$_{10}$)-1,2-*closo*-C$_2$B$_{10}$H$_{10}$}] (**3**) have been assessed by Tolman cone angle and percent buried volume calculations, from which it is concluded that the bis(carboranyl)phosphines **I** and **1** are comparable to PCy$_3$ in their steric demands. The selenides [μ-2,2′-P(Ph)Se-{1-(1′-1′,2′-*closo*-C$_2$B$_{10}$H$_{10}$)-1,2-*closo*-C$_2$B$_{10}$H$_{10}$}] (**4**) and [μ-2,2′-P(Et)Se-{1-(1′-1′,2′-*closo*-C$_2$B$_{10}$H$_{10}$)-1,2-*closo*-C$_2$B$_{10}$H$_{10}$}] (**5**) have also been prepared and characterised. The $^1J_{PSe}$ coupling constants for **4** and **5** are the largest reported so far for carboranylphosphine selenides and indicate that **I** and **1** are very weakly basic.

Introduction

Currently, one of the most active areas of carborane chemistry concerns the compound [1-(1′-1′,2′-*closo*-C$_2$B$_{10}$H$_{11}$)-1,2-*closo*-C$_2$B$_{10}$H$_{11}$], two *ortho*-carborane units connected by a C–C bond[1] and commonly referred to as 1,1′-bis(*o*-carborane) (Fig. 1). Although it was first reported >50 years ago,[2] the chemistry of 1,1′-bis(*o*-carborane) was not fully explored for long periods because of the lack of a reliable, high-yielding synthesis. However, this has now been achieved[3] and consequently a significant amount of new chemistry of 1,1′-bis(*o*-carborane) has recently appeared.[4–20]

Several authors have taken advantage of the functionality of its C$_{cage}$H units to use 1,1′-bis(*o*-carborane) as a κ^2 ligand,

[a]Institute of Chemical Sciences, Heriot-Watt University, Edinburgh, UK EH14 4AS. E-mail: t.kraemer@hw.ac.uk, a.j.welch@hw.ac.uk; Tel: +44 (0)131 451 3259, +44 (0)131 451 3217
[b]Department of Chemistry, University of Bath, Bath, UK BA2 7AY
[c]A. N. Nesmeyanov Institute of Organoelement Compounds, Russian Academy of Sciences, 28 Vavilov Str., 119991 Moscow, Russia

†Dedicated to Professor Evamarie Hey-Hawkins on the occasion of her 60th birthday.
‡Electronic supplementary information (ESI) available: NMR spectra of all new compounds reported. Full details of computational studies. CCDC 1527028–1527033. For ESI and crystallographic data in CIF or other electronic format see DOI: 10.1039/c7dt00485k
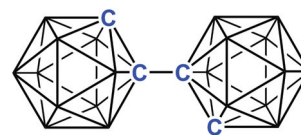

Fig. 1 1,1′-Bis(*o*-carborane).

binding transition-metals to the cage through two M–C σ-bonds, with recent studies[7,8,13,19] building on the pioneering work of Hawthorne and co-workers.[21] In marked contrast, very little has been reported concerning main group elements bound to 1,1′-bis(*o*-carborane). Zakharkin reported [μ-2,2′-AsMe-{1-(1′-1′,2′-*closo*-C$_2$B$_{10}$H$_{10}$)-1,2-*closo*-C$_2$B$_{10}$H$_{10}$}] and [μ-2,2′-PPh-{1-(1′-1′,2′-*closo*-C$_2$B$_{10}$H$_{10}$)-1,2-*closo*-C$_2$B$_{10}$H$_{10}$}] (**I**), although the latter was only poorly characterised,[22,23] and Johnson and Knobler described [μ-2,2′-PX-{1-(1′-1′,2′-*closo*-C$_2$B$_{10}$H$_{10}$)-1,2-*closo*-C$_2$B$_{10}$H$_{10}$}], X = Cl and F.[24] Very recently, Peryshkov and co-workers isolated an interesting 12-vertex closo/12-vertex nido species with both bridging P(*i*-Pr)$_2$ and non-bridging PH(*i*-Pr)$_2$ units when attempting to add two P(*i*-Pr)$_2$ groups onto 1,1′-bis(*o*-carborane), one on each cage.[17]

In this contribution we expand on Zakharkin's early work, resynthesising **I** (in higher yield) and preparing the related μ-2,2′-PEt compound (**1**), with full characterisation of both bis(carboranyl)phosphines. All phosphine have potential as

ligands in homogeneous catalysis, and consequently we have explored the steric and electronic properties of **I** and **1** *via* the synthesis and study of derivatives in which the P lone pair is bound to {–AuCl} and {=Se} fragments.

Results and discussion

Bis(carboranyl)phosphines

Double deprotonation of 1,1'-bis(*o*-carborane) in Et$_2$O with *n*-BuLi in hexanes followed by treatment with PPhCl$_2$ affords [μ-2,2'-PPh-{1-(1'-1',2'-*closo*-C$_2$B$_{10}$H$_{10}$)-1,2-*closo*-C$_2$B$_{10}$H$_{10}$}] (**I**) as a white solid in 72% isolated yield, following work-up involving flash chromatography on silica. Although this bis-(carboranyl)phosphine has been reported before it was previously characterised only by elemental analysis.[22] We have studied the compound by mass spectrometry, multinuclear NMR spectroscopy and single-crystal X-ray diffraction.

The mass spectrum of **I** is dominated by a typical carborane envelope centred at *m/z* 392 corresponding to the molecular ion. The ^{11}B{^{1}H} NMR spectrum contains resonances from δ *ca.* 0 to −13 ppm but is relatively uninformative in terms of the detailed structure because of the overlap of the lower-frequency resonances. The ^{1}H NMR spectrum confirms that no C$_{cage}$*H* resonances are present and reveals the expected multiplets for ortho, meta and para H atoms which collapse to a doublet, apparent triplet and triplet, respectively, on ^{31}P decoupling. In the ^{31}P{^{1}H} spectrum there is a simple singlet at δ 40.35 ppm.

The molecular structure of **I** is shown in Fig. 2. As anticipated the {PPh} fragment binds symmetrically to the bis-(carborane) (the P1–C2 and P1–C2' distances are identical within experimental error), and only a small rotation of the Ph substituent about the P1–C11 bond would afford the molecule C_s symmetry, the likely time-averaged symmetry in solution.
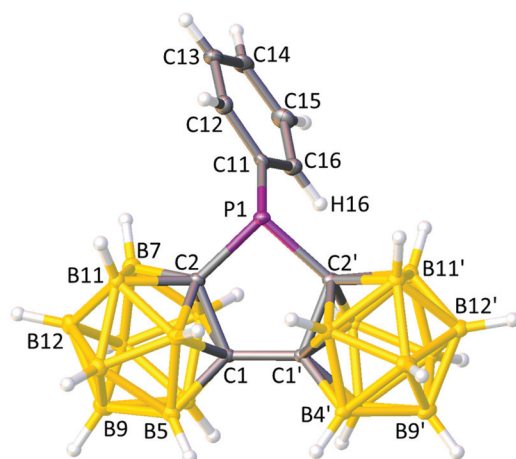
The formation of the P1C2C1C1'C2' ring results in a slight bending of the spine of the bis(carborane) with angles B12···C1–C1' 169.14(16)° and B12'···C1'–C1 170.17(15)°, *cf.* 175.14(5)° in 1,1'-bis(*o*-carborane) itself.[1]

An analogous compound, [μ-2,2'-PEt-{1-(1'-1',2'-*closo*-C$_2$B$_{10}$H$_{10}$)-1,2-*closo*-C$_2$B$_{10}$H$_{10}$}] (**1**), was similarly prepared. The ^{11}B{^{1}H} NMR spectrum of **1** reveals a 2 : 2 : 6 : 2 : 2 : 6 pattern (high frequency to low frequency) between δ *ca.* 0 and −11 ppm, consistent with time-averaged C_s molecular symmetry. The ^{1}H{^{31}P} NMR spectrum affords the expected quartet and triplet for the PC*H*$_2$CH$_3$ and PCH$_2$C*H*$_3$ resonances, respectively, and a singlet at δ 42.75 ppm is observed in the ^{31}P{^{1}H} spectrum.

There are two crystallographically-independent molecules of compound **1** in the asymmetric fraction of the unit cell, and Fig. 3 shows a perspective view of one of them, **1**AB (the other is **1**CD). Using the *Structure Overlay* tool in Mercury[25] the overall root-mean-square (rms) misfit between the {P(C$_2$B$_{10}$)$_2$} fragments of the two independent molecules (25 atoms) is 0.024 Å, with the greatest individual misfit between B4B and B4D, 0.049 Å. Including the C atoms of the Et groups results in only a marginal increase in the rms misfit to 0.029 Å (the greatest individual misfit 0.073 Å between C12A and C12C) since the orientation of the ethyl group relative to the bis(carborane) in the two independent molecules is effectively the same.

This ethyl orientation is significant because of its influence on the ^{1}H NMR spectroscopic properties of **1** (*vide infra*). We believe that the origin of the orientation is that it maximises intramolecular dihydrogen bonding between the weakly protonic C*H* atoms and the weakly hydridic B*H* atoms of the carborane cage, with the key CH···HB contacts shown in Fig. 4, an alternative view of **1**AB.

Fig. 2 Perspective view of **I** with the atomic numbering scheme. Displacement ellipsoids are drawn at the 50% probability level except for H atoms. Selected interatomic distances (Å): P1–C2 1.893(3), P1–C2' 1.887(3), P1–C11 1.819(3), and C1–C1' 1.534(3).
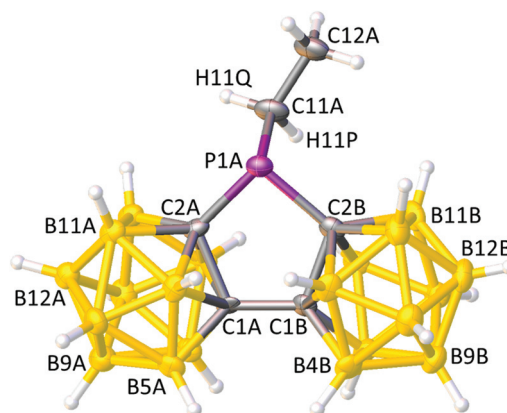

Fig. 3 Perspective view of one of the two crystallographically-independent molecules of compound **1** (**1**AB) with the atomic numbering scheme. Molecule **1**CD is practically superimposable. Displacement ellipsoids are as in Fig. 2. Selected interatomic distances (Å): P1A–C2A 1.870(5), P1A–C2B 1.890(5), P1A–C11A 1.844(5), C1A–C1B 1.533(7); P1C–C2C 1.886(5), P1C–C2D 1.890(5), P1C–C11C 1.818(5), and C1C–C1D 1.530(6).
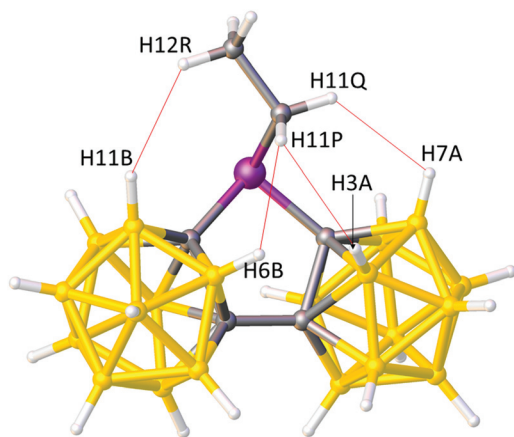
Fig. 4 Alternative view of **1**AB showing dihydrogen bonds as red lines. Interatomic distances (Å): H11P···H3A 2.45(4), *2.39(4)*, **2.28**; H11P···H6B 2.28(5), *2.29(5)*, **2.10**; H11Q···H7A 2.46(5), *2.47(4)*, **2.36**; H12R···H11B 2.51(5), *2.40(5)*, **2.31**. Values in *italics* are the equivalent distances in molecule **1**CD, and values in **bold** are those from the DFT study of **1**.

To investigate this further we have undertaken DFT calculations on compound **1**. The optimised (BP86-D3/def2-TZVP/def2-SVP) geometry, **1**$_{DFT}$ (Fig. 5), is in excellent agreement with the structure determined crystallographically (see the ESI‡ for key optimised bond parameters), including the orientation of the ethyl group. Thus the overall rms misfit between the computed and experimental {P(C₂B₁₀)₂} fragments (using molecule **1**AB) is only 0.019 Å (the greatest individual misfit 0.031 Å for P1), rising to only 0.029 Å if the ethyl C atoms are included (the greatest individual misfit 0.081 Å for C12A). In terms of the ethyl group orientation, the experimental lp–P1–C11–C12 torsion angles are 38.8(4)° and 42.5(4)° for **1**AB and **1**CD, respectively, and the computed torsion angle is 38.4°. Moreover, the DFT study provides strong support for the presence of dihydrogen bonding. A topological analysis of the electron density in **1**$_{DFT}$ using the QTAIM methodology reveals
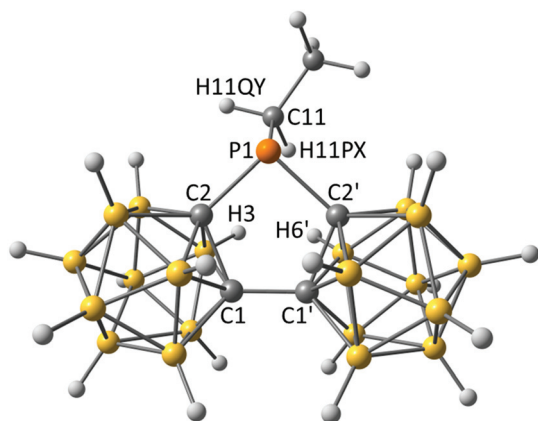

Fig. 5 DFT-optimised structure of **1**. Note the excellent agreement with the experimentally-determined structure (Fig. 3), including the orientation of the Et group. Selected interatomic distances (Å): P1–C2 1.889, P1–C2′ 1.892, P1–C11 1.852, and C1–C1′ 1.528.

bond critical points (BCP) between H11PX and the cage hydrogen atoms H3 and H6′, located roughly at the centre of each bond vector (see Fig. S1‡ for a molecular graph). Additional, albeit somewhat weaker interactions, are present for H11QY/H7 and H12R/H11 (see Fig. S1‡). Both the electron density $\rho(r)$ (0.007–0.011 a.u.) and its Laplacian $\nabla^2\rho(r)$ (0.022–0.038 a.u.) at the relevant BCPs are diagnostic of typical closed-shell interactions and fall within the ranges proposed for dihydrogen bonds.[26]

An interesting feature of the ^{1}H NMR spectrum of compound **1** is the lack of observable coupling between the PCH_2CH$_3$ H atoms and the P atom. Thus, whilst the PCH$_2$CH_3 H atoms appear as a doublet (${}^3J_{PH}$ = 23.0 Hz) of triplets (${}^3J_{HH}$ = 7.9 Hz) the PCH_2CH$_3$ H atoms appear as only a simple quartet (${}^3J_{HH}$ = 7.9 Hz). A ^{1}H–^{31}P HMBC experiment shows the presence of the expected coupling between the P atom and the CH$_2$CH_3 H atoms but, additionally, a weak correlation between signals due to P and CH_2CH$_3$. The lack of any observable splitting in the 1D ^{1}H spectrum suggests that the value of ${}^2J$ (^{1}H–^{31}P) is of the order of the ^{1}H resonance linewidth (estimated to be *ca.* 1 Hz).

An understanding of the origin of this small 2-bond P–H coupling comes from the DFT calculations on compound **1**. The computed energy profile for ethyl rotation about the P1–C11 vector (Fig. 6) establishes that **1**$_{DFT}$ and its isoenergetic rotational conformer **1**′$_{DFT}$ dominate the equilibrium distribution, whilst the Boltzmann population of the symmetrical isomer **1**″$_{DFT}$ (+4 kcal mol⁻¹) is near zero at room temperature. Importantly, due to the low energetic barrier associated with **TS(1$_{DFT}$–1**′$_{DFT}$**)** separating **1**$_{DFT}$ and **1**′$_{DFT}$ ($\Delta G^\ddagger$ = +1.8 kcal mol⁻¹) the methylene protons can undergo rapid exchange in solution. The calculated averaged ${}^3J_{PH}$ (calc. 26.2 Hz; exp. 23.0 Hz) and ${}^3J_{HH}$ (calc. 9.7 Hz; exp. 7.9 Hz) coupling constants are in good agreement with the experimental values. The values of ${}^2J_{PH}$ for coupling to the individual methylene hydrogen atoms are of the same order of magnitude but, importantly, they are of opposite sign (for H11PX ${}^2J_{PH}$ = −5.4 Hz whilst for H11QY ${}^2J_{PH}$ = +5.6 Hz). Hence, fast exchange between these hydrogen atoms reduces the observed ${}^2J_{PH}$ to approximately zero, in line with the experimental upper limit of ~±1 Hz. The predominant contribution to the total coupling constant is associated with the Fermi contact term.

With the characterisation of **I** and **1** now complete, we turn to their derivatives. Phosphines are ligands of great importance in homogeneous catalysis by transition-metal complexes,[27] and carboranylphosphines have been used extensively in a variety of catalytic applications.[28] The two key characteristics of phosphines as ligands in catalysis are their size and basicity, and we have targeted and studied derivatives of **I** and **1** specifically to assess these features.

Steric properties

The steric demand of a phosphine is classically assessed using its Tolman cone angle (θ),[29] and we have used the crystallographically-determined structures of **I** and **1** to measure these. In addition, a recent alternative to θ is Cavallo and Nolan's
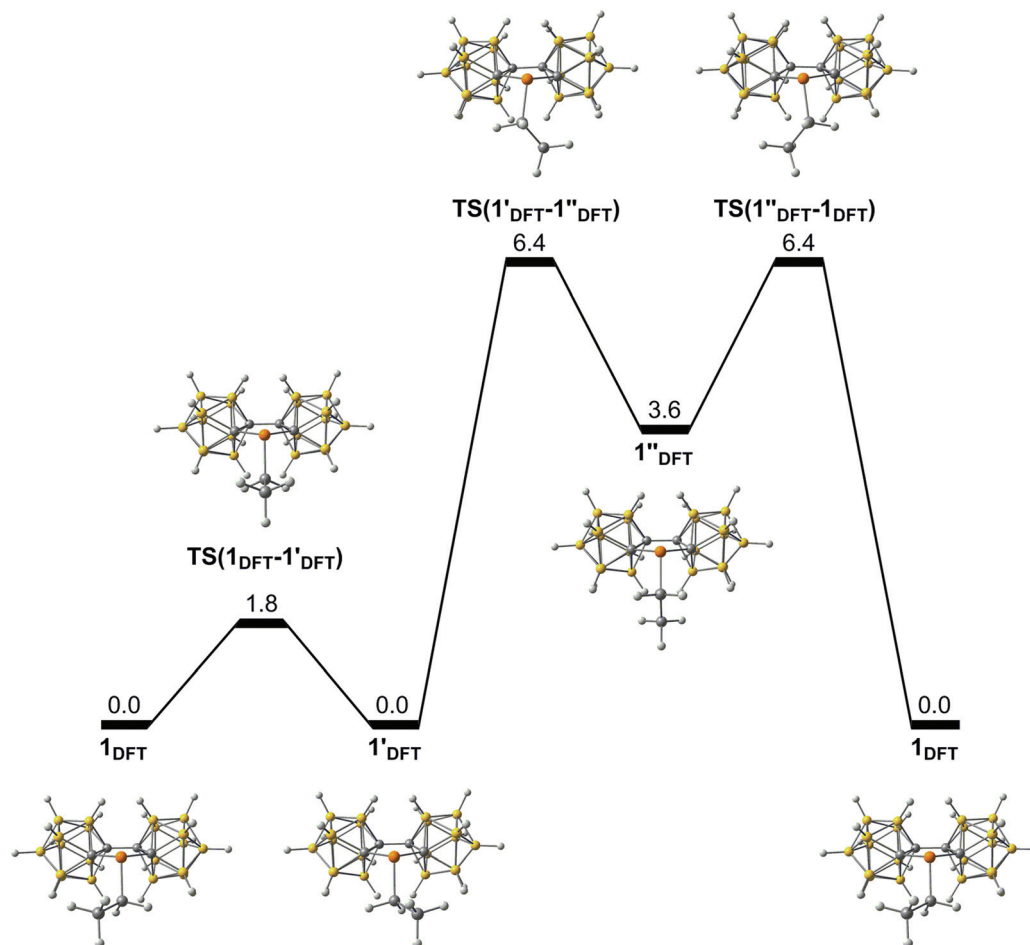
Fig. 6 Calculated Gibbs free energy profile (kcal mol^{-1}) for ethyl rotation in 1_{DFT} (BP86-D3/def2-TZVP/def2-SVP). Boltzmann populations: 1_{DFT} 50%, $1'_{DFT}$ 50%, and $1''_{DFT}$ 0%.

percent buried volume parameter, %V_{bur}.[30] Although originally developed for NHCs, %V_{bur} has been shown to scale linearly with θ for a range of phosphines and, furthermore, there is a strong linear relationship between θ of PR$_3$ and %V_{bur} of the adduct R$_3$PAuCl.[31] For this reason we have prepared and studied the gold–chloride adducts of compounds **I** and **1**.

Treatment of a solution of **I** or **1** in DCM with an equimolar amount of (tht)AuCl affords the new species [μ-2,2′-P(Ph)AuCl-{1-(1′-1′,2′-*closo*-C$_2$B$_{10}$H$_{10}$)-1,2-*closo*-C$_2$B$_{10}$H$_{10}$}] (**2**) and [μ-2,2′-P(Et)AuCl-{1-(1′-1′,2′-*closo*-C$_2$B$_{10}$H$_{10}$)-1,2-*closo*-C$_2$B$_{10}$H$_{10}$}] (**3**) as white solids in 81 and 32% yields, respectively.

Compounds **2** and **3** were initially characterised by mass spectrometry and ^{1}H, ^{11}B and ^{31}P NMR spectroscopies. The ^{11}B{^{1}H} spectrum of **2** is largely uninformative because of multiple overlapping resonances, but that of **3** is sufficiently well-resolved to allow integration, which is consistent with time-averaged C_s molecular symmetry in solution at room temperature. In both **2** and **3** the ^{31}P{^{1}H} spectrum reveals a simple singlet, shifted *ca.* 28 and 33 ppm, respectively, to a high frequency relative to those in **I** and **1**. The ^{1}H NMR spectrum of **2** shows the anticipated multiplets for the phenyl protons,

whilst for **3** the H atoms of the ethyl group appear as a doublet of quartets (PCH_2CH$_3$) and a doublet of triplets (PCH$_2$CH_3).

The molecular structures of **2** and **3**, as determined crystallographically, are shown in Fig. 7 and 8, respectively. In both cases co-ordination to the {AuCl} fragments causes minimal change in the structures of the bis(carboranyl)phosphines, with the same orientations of the Ph groups or Et groups being effectively maintained between **I** and **2** and between **1** and **3**. Moreover, a DFT-optimised study of **3** was fully consistent with its crystallographic counterpart; a structure overlay of **3** and **3**$_{DFT}$ yielded an overall rms misfit of 0.018 Å for {P(C$_2$B$_{10}$)$_2$} fragments (the greatest individual misfit 0.027 Å for B5′) rising to only 0.020 Å if the ethyl carbon atoms were included (the greatest misfit 0.033 Å for C11). The overlay is somewhat poorer if the {AuCl} fragment is included, with the overall misfit increasing to 0.077 Å and the Cl atoms misfitting by 0.345 Å.

The Tolman cone angle for **I** was calculated to be 172.5°, whilst that for **1** is 171.6° (Table 1). Although Ph is a larger substituent than Et, the similarity of the cone angles for **I** and **1** reflects the fact that the vast majority of the steric bulk of
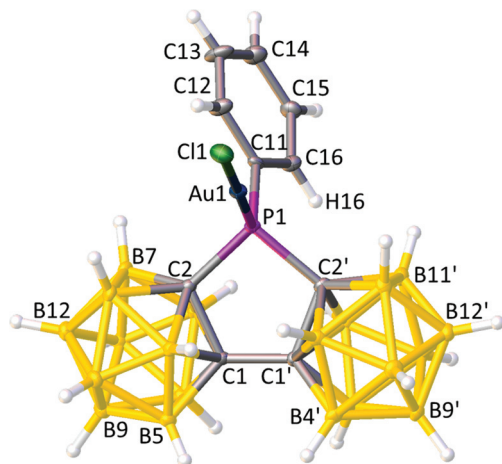
Fig. 7 Perspective view of compound **2** with the atomic numbering scheme. Displacement ellipsoids are as in Fig. 2. Selected interatomic distances (Å): P1–Au1 2.2217(8), Au1–Cl1 2.2698(8), P1–C2 1.878(3), P1–C2′ 1.879(3), P1–C11 1.797(3), and C1–C1′ 1.523(4).
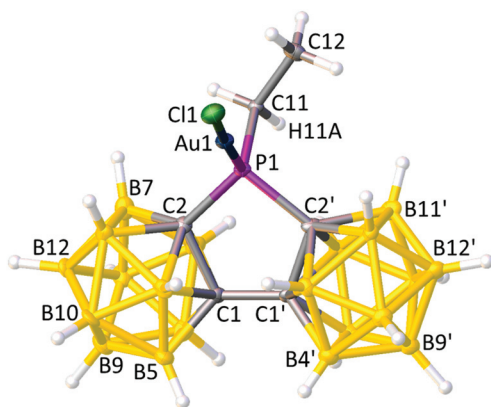

Fig. 8 Perspective view of compound **3** with the atomic numbering scheme. Displacement ellipsoids are as in Fig. 2. Selected interatomic distances (Å): P1–Au1 2.2181(11), Au1–Cl1 2.2910(11), P1–C2 1.860(4), P1–C2′ 1.883(4), P1–C11 1.816(4), and C1–C1′ 1.538(5).

Table 1 Tolman cone angles (θ/°) and %V_{bur} for bis(carboranyl)phosphines **I** and **1** and their complexes with {AuCl}, **2** and **3** respectively

	θ	%V_{bur}
I	172.5	32.0
1AB	171.6	30.9
1CD	171.6	30.7
2	176.2	33.2
3	176.5	32.0

I and **1** comes from the common bis(carborane) fragment. Percent buried volumes for **I** and **1** were calculated to be 32.0 and 30.8 (average), respectively. Co-ordination to {AuCl} to afford **2** and **3**, respectively, results in small increases in both θ and %V_{bur}. This arises because the stereochemical influence of the P lone pair of electrons on the bis(carborane) and Ph/Et sub-

stituents is reduced on co-ordination, allowing small increases in the C–P–C angles and producing a slightly bulkier ligand.

Comparing the θ and %V_{bur} values for **I**, **1**, **2** and **3** with analogous species in the literature, we conclude that the bis(carboranyl)phosphines **I** and **1** are, in terms of their size, the most comparable to (but slightly larger than) tricyclohexylphosphine, PCy$_3$.[31]

Electronic properties

The basicity of phosphines PR$_3$ is conveniently assessed by the measurement of the 1-bond P–Se coupling constant, $^1J_{PSe}$, of the corresponding selenide R$_3$P=Se; the more electron-withdrawing the substituents (*i.e.* the less basic the phosphine), the greater the degree of 3s character in the phosphorus lone pair and the greater the magnitude of $^1J_{PSe}$.[32] Accordingly, we have synthesised [μ-2,2′-P(Ph)Se-{1-(1′-1′,2′-*closo*-C$_2$B$_{10}$H$_{10}$)-1,2-*closo*-C$_2$B$_{10}$H$_{10}$}] (**4**) and [μ-2,2′-P(Et)Se-{1-(1′-1′,2′-*closo*-C$_2$B$_{10}$H$_{10}$)-1,2-*closo*-C$_2$B$_{10}$H$_{10}$}] (**5**), the selenides of **I** and **1** respectively, by the simple process of heating the bis(carboranyl)phosphine with an excess of elemental Se in toluene. Scheme 1 summarises all the syntheses reported in this paper.

Compounds **4** and **5** are afforded as pale-pink solids in reasonable isolated yields. Both show the anticipated molecular ion peaks in their mass spectra. Their ^{11}B{^{1}H} NMR spectra are relatively uninformative due to considerable overlap of resonances. In the ^{31}P{^{1}H} NMR spectra are singlets at δ *ca.* 50 and 58 ppm, respectively, at higher frequency than in the corresponding bis(carboranyl)phosphine but not as deshielded as in the AuCl compounds **2** and **3**. The ^{1}H NMR spectra of **4** and **5** show the expected resonances for the Ph or Et substituents, including a doublet of quartets for the PCH_2CH$_3$ resonance of **5** with $^2J_{PH}$ = 11.6 Hz, and the re-emergence of this 2-bond P–H coupling can be understood in terms of the rehybridisation of the phosphorus orbitals induced by coordination of the P lone pair to the {=Se} fragment.[33] These changes closely follow the general trends observed for P(III) and P(V) compounds.[34] The computed averaged geminal $^2J_{PH}$ coupling constant in **5$_{DFT}$** increases to −14.1 Hz, a value in good agreement with experiment ($^2J_{PH}$ = 11.6 Hz). We note that the phase information of the coupling constant is invisible in first-order NMR-spectra, and thus all coupling constants appear to be positive. The observed decrease of $^2J_{PH}$ (or increase of the modulus $|^2J_{PH}|$) can be correlated with the admixture of a higher degree of 3s character into the P bonds, rendering the hybridisation around P close to sp^3, as borne out in the NBO analysis of the associated P–C bonding orbitals (21–26% s, 73–78% p). This is paralleled by a notable reduction of P 3s character in the P–Se σ-bond (32% s, 67% p), compared to 52% 3s character of the phosphorus lone pair in **1$_{DFT}$**. This change of the electron distribution around P as the lone pair is replaced by Se in **5$_{DFT}$** in turn reinforces the direct Fermi contact contribution to the 1- and 2-bond coupling pathways (see the ESI‡ for more details).

Of relevance to the basicities of the bis(carboranyl)phosphine parent compounds **I** and **1**, the ^{31}P{^{1}H} spectra of **4** and **5** show clear Se satellites with $^1J_{PSe}$ = 891 and 894 Hz, respect-
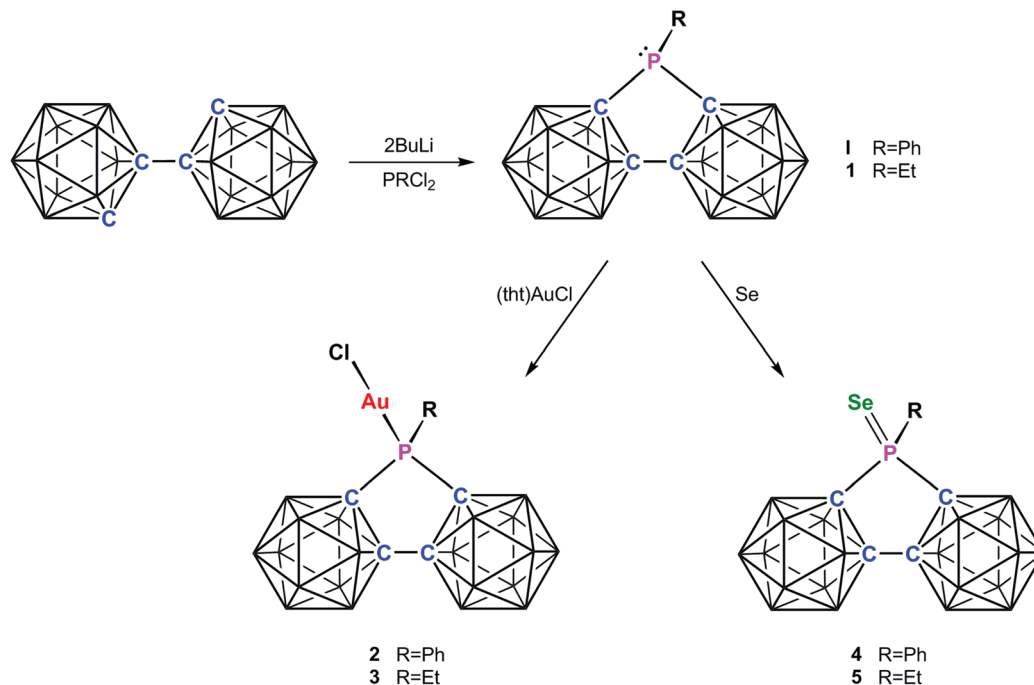
Scheme 1 Generalised reaction scheme for compounds **I** and **1–5**.

ively.[35] These coupling constants are considerably larger than those of a range of common phosphines [typically 670–750 Hz, Table 1 of ref. 32d], suggesting that **I** and **1** are very weakly basic. There are few carboranylphosphine selenides in the literature, but those that are known all have relatively large values of $^1J_{PSe}$. In [1-P(Se)Ph$_2$-2-PPh$_2$-1,2-$closo$-C$_2$B$_{10}$H$_{10}$] $^1J_{PSe}$ = 807 Hz, whilst in the 2-Me and 2-Ph analogues $^1J_{PSe}$ = 804 and 812 Hz, respectively.[36] Clearly, these large couplings are the result of the strong electron-withdrawing property of carboranes relative to alkyl or aryl substituents, and we attribute the even larger $^1J_{PSe}$ values in **4** and **5** to the fact that here the

{P=Se} fragment is directly bonded to two carborane cages. Consistent with this, Viñas and co-workers have described species [μ-1,1′-P(R)Se-3,3′-Co(1,2-C$_2$B$_9$H$_{10}$)$_2$]$^-$ in which the {P(R)Se} fragment is also attached to two heteroborane cages and reported $^1J_{PSe}$ values of 833 Hz (R = Ph) and 679 Hz (R = t-Bu).[37] In the related species [8,8′-μ-(1″,2″-C$_6$H$_4$)-μ-1,1′-P(R)Se-3,3′-Co(1,2-C$_2$B$_9$H$_9$)$_2$]$^-$, $^1J_{PSe}$ is 848 Hz (R = Ph) and 692 Hz (R = t-Bu), respectively.[37]

Overall, the magnitudes of $^1J_{PSe}$ recorded for **4** and **5** are currently the largest reported for carboranylphosphine selenides, implying that the parent phosphines **I** and **1** are very weakly basic. Note that, in principle, the degree of s character
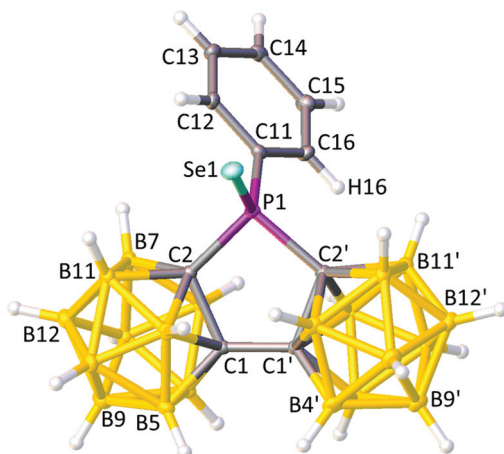

Fig. 9 Perspective view of compound **4** with the atomic numbering scheme. Displacement ellipsoids are as in Fig. 2. Selected interatomic distances (Å): P1–Se1 2.0798(6), P1–C2 1.8860(19), P1–C2′ 1.896(2), P1–C11 1.810(2), and C1–C1′ 1.536(3).
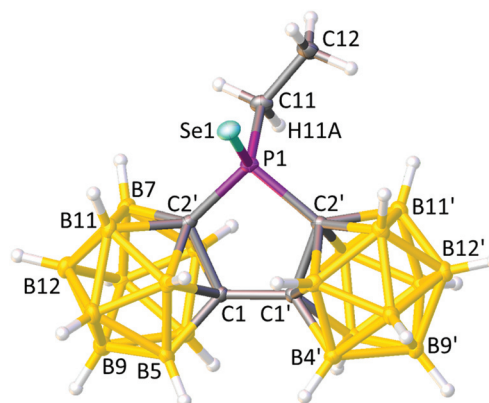

Fig. 10 Perspective view of compound **5** with the atomic numbering scheme. Displacement ellipsoids are as in Fig. 2. Selected interatomic distances (Å): P1–Se1 2.0801(7), P1–C2 1.879(2), P1–C2′ 1.893(2), P1–C11 1.822(2), and C1–C1′ 1.543(3).

Table 2 X–P–C11–C12 torsion angles (/°) and key dihydrogen bonding (/Å) in bis(carboranyl)phosphines and related compounds

Compound	X	X–P–C11–C12	Dihydrogen bond	Distance	Dihydrogen bond	Distance
(i) Phenyl substituent						
I	lp	−29.4(2)	H16···H6′	2.15(3)	H16···H3	2.48(2)
2	Au	−28.8(3)	H16···H6′	2.20(3)	H16···H3	2.49(3)
4	Se	−40.0(2)	H16···H6′	2.19(2)	H16···H3	2.84(2)
(ii) Ethyl substituent						
1AB	lp	38.8(4)	H11P···H6B	2.28(5)	H11P···H3A	2.45(5)
1CD	lp	42.5(4)	H11X···H6D	2.29(5)	H11X···H3C	2.39(4)
1$_{DFT}$	lp	38.4	H11PX···H6′	2.10	H11PX···H3	2.28
3	Au	37.7(3)	H11A···H6′	2.32(3)	H11A···H3	2.52(4)
3$_{DFT}$	Au	39.8	H11A···H6′	2.17	H11A···H3	2.34
5	Se	48.6(3)	H11A···H6′	2.40(3)	H11A···H3	2.46(2)
5$_{DFT}$	Se	39.9	H11A···H6′	2.14	H11A···H3	2.29

in the phosphorus lone pair in PR_3 can be influenced not only by the electron-withdrawing properties but also by the size of the substituents. In this respect we recall that **I** and **1** are comparable in their steric demands to PCy_3. They are, however, much less basic, since $^1J_{PSe}$ in $Cy_3P\text{=}Se$ is only 673 Hz.[38]

Compounds **4** and **5** were also studied crystallographically, and perspective views of single molecules are shown in Fig. 9 and 10, respectively. As noted above, compound **5** was also studied computationally, again affording excellent agreement with the crystallographic structure; for the $\{P(C_2B_{10})_2\}$ fragments of **5** and **5$_{DFT}$** the rms misfit is 0.020 Å (the worst individual misfit 0.034 Å for B11′), rising to only 0.034 Å (the poorest individual fit 0.100 Å for C11) when the ethyl C atoms are included and 0.036 Å (the worst fit 0.098 Å, C12) when the Se atom is added. Once again, the general orientation of the Ph or Et substituent relative to the bis(carborane) moiety is maintained, with torsion angles lp/Au/Se–P–C11–C12 broadly consistent for **I**, **2** and **4** (Ph substituents) and for **1**, **1$_{DFT}$**, **3**, **3$_{DFT}$**, **5** and **5$_{DFT}$** (Et substituents) albeit with a *ca.* 10° increase for the selenides **4** and **5** (Table 2). As previously noted, for the ethyl species **1**, **3** and **5** this orientation is traced to intramolecular dihydrogen bonding involving H11A (H11P and H11X in **1**) with H6′ and with H3, whilst for the phenyl compounds **I**, **2** and **4** H16 of the phenyl ring is seen to interact primarily with H6′ and to a lesser extent with H3.

The P=Se distances in **4** and **5** are 2.0798(6) and 2.0801(7) Å, respectively. These are significantly shorter than that in $Cy_3P\text{=}Se$, 2.108(1) Å,[39] and those in recent compilations of P=Se distances.[38,40] In fact, the P=Se distances in **4** and **5** are amongst the shortest yet reported; of 378 structures containing the fragment $\{R^1R^2R^3P\text{=}Se\}$ in the Cambridge Structural Database[41] only seven have P=Se distances <2.08 Å.[42] Short P=Se distances in **4** and **5** are fully consistent with a significant degree of s character in the phosphorus lone pair of **I** and **1**, as implied from the $^1J_{PSe}$ values.

Conclusions

The bis(carboranyl)phosphines **I** and **1** are comparable in their steric demands to PCy_3 but are much less basic. In fact, in terms of their $^1J_{PSe}$ values, **I** and **1** are the least basic of any carboranylphosphines so far reported. As large, weakly basic phosphines **I** and **1** have potential as ligands in homogeneous catalysis, and future contributions will develop this theme.

Experimental

Synthesis

Experiments were performed under dry, oxygen free N_2 using standard Schlenk techniques, although subsequent manipulations were sometimes performed in an open laboratory. Solvents were either freshly distilled under nitrogen from the appropriate drying agent [THF, Et_2O and 40–60 °C petroleum ether (petrol); sodium wire: CH_2Cl_2 (DCM); calcium hydride] or were purified by using an MBRAUN SPS-800 and stored over 4 Å molecular sieves, and all were degassed (3× freeze–pump–thaw cycles) before use. Preparative TLC employed 20 × 20 cm Kieselgel F_{254} glass plates and for column chromatography we used 60 Å silica as the stationary phase. NMR spectra at 400.1 MHz (^1H), 128.4 MHz (^{11}B) or 162.0 MHz (^{31}P) were recorded on a Bruker DPX-400 spectrometer from $CDCl_3$ solutions at 298 K, using $CDCl_3$ stored over 4 Å molecular sieves. Electron impact mass spectrometry (EIMS) was carried out using a Finnigan (Thermo) LCQ Classic ion trap mass spectrometer (University of Edinburgh). The starting materials 1,1′-bis(*o*-carborane)[3] and (tht)AuCl[43] were prepared by literature methods or slight variations thereof. All other reagents were supplied commercially.

[μ-2,2′-PPh-{1-(1′-1′,2′-*closo*-C$_2$B$_{10}$H$_{10}$)-1,2-*closo*-C$_2$B$_{10}$H$_{10}$}] (I). *n*-BuLi (2.79 mL of 2.5 M solution in hexanes, 6.975 mmol) was added dropwise to a cooled (0 °C) solution of 1,1′-bis (*o*-carborane) (1.000 g, 3.491 mmol) in Et_2O (20 mL) and the products were stirred for 1 h at room temperature. The pale yellow solution was cooled to 0 °C and then $PPhCl_2$ (0.47 mL, 3.491 mmol) in Et_2O (10 mL) was added over 30 min to afford a green-yellow solution, which was subsequently heated to reflux for 2 h to produce a pale yellow solution. Once cooled this was filtered and the solvent was removed *in vacuo*. Purification by flash chromatography (petrol) yielded a white solid, subsequently identified as [μ-2,2′-PPh-{1-(1′-1′,2′-*closo*-

$C_2B_{10}H_{10})$-1,2-$closo$-$C_2B_{10}H_{10}$}] **(I)** (0.981 g, 2.499 mmol, 72%). $^{11}B\{^1H\}$ NMR, δ −0.1 (2B), −3.9 to −11.2 [overlapping resonances with maxima at −3.9, −6.4, −8.7, −9.8, −11.2 (18B)]. ^1H NMR, δ 7.77–7.73 (m, 2H, C_6H_5), 7.65–7.62 (m, 1H, C_6H_5), 7.59–7.54 (m, 2H, C_6H_5). $^1H\{^{31}P\}$ NMR, δ 7.76 (d, $^3J_{HH}$ = 7.1 Hz, 2H, C_6H_5), 7.64 (t, $^3J_{HH}$ = 7.4 Hz, 1H, C_6H_5), 7.57 (app t, $^3J_{HH}$ = 7.1 Hz, 2H, C_6H_5). $^{31}P\{^1H\}$ NMR, δ 40.35 (s). EIMS, envelope centred on m/z 392.3 (M$^+$).

[μ-2,2′-PEt-{1-(1′-1′,2′-$closo$-$C_2B_{10}H_{10}$)-1,2-$closo$-$C_2B_{10}H_{10}$}] (1). n-BuLi (0.56 mL of a 2.5 M solution in hexanes, 1.396 mmol) was added dropwise to a cooled (0 °C) solution of 1,1′-bis (o-carborane) (0.200 g, 0.698 mmol) in THF (10 mL) and the products were stirred for 1 h. The pale yellow solution was frozen at −196 °C and then PEtCl$_2$ (0.70 mL of a 1.0 M solution in THF, 0.698 mmol) was added and the reaction mixture was stirred overnight at room temperature to give a colourless solution. Volatiles were removed *in vacuo* and the crude mixture was dissolved in DCM and filtered. Purification by flash chromatography (petrol) followed by preparative TLC (DCM : petrol, 1 : 19) yielded a white solid (R_f = 0.97), subsequently identified as [μ-2,2′-PEt-{1-(1′-1′,2′-$closo$-$C_2B_{10}H_{10}$)-1,2-$closo$-$C_2B_{10}H_{10}$}] **(1)** (0.154 g, 0.447 mmol, 64%). $^{11}B\{^1H\}$ NMR, δ −0.3 (2B), −3.8 (2B), −6.6 (6B), −7.6 (2B), −8.5 (2B), −10.6 (6B). ^1H NMR, δ 1.98 (q, 2H, PCH_2CH$_3$, $^3J_{HH}$ = 7.9 Hz), 1.31 (dt, 3H, PCH$_2$CH_3, $^3J_{HH}$ = 7.9 Hz, $^3J_{PH}$ = 23.0 Hz). $^1H\{^{31}P\}$ NMR, δ 1.99 (q, 2H, PCH_2CH$_3$, $^3J_{HH}$ = 7.9 Hz), 1.32 (t, 3H, PCH$_2$CH_3, $^3J_{HH}$ = 7.9 Hz). $^{31}P\{^1H\}$ NMR, δ 42.75 (s). EIMS, envelope centred on m/z 344.3 (M$^+$).

[μ-2,2′-P(Ph)AuCl-{1-(1′-1′,2′-$closo$-$C_2B_{10}H_{10}$)-1,2-$closo$-$C_2B_{10}H_{10}$}] (2). A DCM (5 mL) solution of **I** (0.100 g, 0.255 mmol) was transferred *via* a cannula to a DCM (10 mL) solution of (tht) AuCl (0.082 g, 0.256 mmol) at 0 °C. The colourless solution was stirred at 0 °C for 30 min, and then reduced to *ca.* 3 mL *in vacuo.* Petrol (10 mL) was added to afford a white precipitate which was collected by filtration and washed with petrol (10 mL) to give a white solid, subsequently identified as [μ-2,2′-P(Ph)AuCl-{1-(1′-1′,2′-$closo$-$C_2B_{10}H_{10}$)-1,2-$closo$-$C_2B_{10}H_{10}$}] **(2)** (0.129 g, 0.206 mmol, 81%). $^{11}B\{^1H\}$ NMR, δ −1.87 (2B), −0.7 to −13.9 [overlapping resonances with maxima at −3.6, −5.6, −7.6, −9.2, −10.9 (18B)]. ^1H NMR, δ 8.15–8.09 (m, 2H, C_6H_5), 7.86–7.81 (m, 1H, C_6H_5), 7.75–7.70 (m, 2H, C_6H_5). $^{31}P\{^1H\}$ NMR, δ 68.96 (s). EIMS, envelope centred on m/z 624.1 (M$^+$).

[μ-2,2′-P(Et)AuCl-{1-(1′-1′,2′-$closo$-$C_2B_{10}H_{10}$)-1,2-$closo$-$C_2B_{10}H_{10}$}] (3). Similarly, from compound **1** (0.100 g, 0.290 mmol) and (tht)AuCl (0.093 g, 0.290 mmol) was isolated [μ-2,2′-P(Et)AuCl-{1-(1′-1′,2′-$closo$-$C_2B_{10}H_{10}$)-1,2-$closo$-$C_2B_{10}H_{10}$}] **(3)** (0.053 g, 0.092 mmol, 32%) as a white solid. $^{11}B\{^1H\}$ NMR, δ 1.7 (2B), −3.3 (2B), −5.7 (6B), −7.6 (4B), −10.4 (6B). ^1H NMR, δ 2.48 (dq, 2H, PCH_2CH$_3$, $^2J_{PH}$ = 10.9 Hz, $^3J_{HH}$ = 7.7 Hz), 1.52 (dt, 3H, PCH$_2$CH_3, $^3J_{PH}$ = 27.9 Hz, $^3J_{HH}$ = 7.7 Hz). $^{31}P\{^1H\}$ NMR, δ 75.76 (s). EIMS, envelope centred on m/z 577.3 (M$^+$).

[μ-2,2′-P(Ph)Se-{1-(1′-1′,2′-$closo$-$C_2B_{10}H_{10}$)-1,2-$closo$-$C_2B_{10}H_{10}$}] (4). Elemental selenium (0.201 g, 2.546 mmol) was added to a toluene (10 mL) solution of **I** (0.100 g, 0.225 mmol) which was then heated to reflux for 72 h. Excess selenium was removed by filtration and $^{31}P\{^1H\}$ NMR spectroscopy revealed a

74% conversion of **I** to a new species. Preparative TLC (DCM : petrol, 1 : 9) yielded a colourless band at R_f = 0.59 from which the product, [μ-2,2′-P(Ph)Se-{1-(1′-1′,2′-$closo$-$C_2B_{10}H_{10}$)-1,2-$closo$-$C_2B_{10}H_{10}$}] **(4)**, was isolated as a pale-pink solid (0.057 g, 0.120 mmol, 47%). $^{11}B\{^1H\}$ NMR, δ 1.2 (2B), −4.1 to −11.2 [overlapping resonances with maxima at −4.1, −6.0, −6.4, −8.5, −9.9, −11.2 (18B)]. ^1H NMR, δ 8.31–8.25 (m, 2H, C_6H_5), 7.73–7.68 (m, 1H, C_6H_5), 7.63–7.57 (m. 2H, C_6H_5). $^{31}P\{^1H\}$ NMR, δ 50.52 (s + Se satellites, $^1J_{PSe}$ = 891 Hz). EIMS, envelope centred on m/z 471.3 (M$^+$).

[μ-2,2′-P(Et)Se-{1-(1′-1′,2′-$closo$-$C_2B_{10}H_{10}$)-1,2-$closo$-$C_2B_{10}H_{10}$}] (5). Similarly, from Se (0.241 g, 3.052 mmol) and compound **1** (0.100 g, 0.145 mmol) was prepared [μ-2,2′-P(Et)Se-{1-(1′-1′,2′-$closo$-$C_2B_{10}H_{10}$)-1,2-$closo$-$C_2B_{10}H_{10}$}] **(5)**, a pale-pink solid (71% conversion by $^{31}P\{^1H\}$ NMR, isolated yield 0.049 g, 0.116 mmol, 38%). $^{11}B\{^1H\}$ NMR, δ 0.9 (2B), −3.7 (2B), −6.2 to −10.6 [overlapping resonances with maxima at −6.2, −7.6, −8.7, −9.2, −10.6 (16B)]. ^1H NMR, δ 2.72 (dq, 2H, PCH_2CH$_3$, $^2J_{PH}$ = 11.6 Hz, $^3J_{HH}$ = 7.6 Hz), 1.52 (dt, 3H, PCH$_2$CH_3, $^3J_{PH}$ = 25.9 Hz, $^3J_{HH}$ = 7.6 Hz). $^{31}P\{^1H\}$ NMR, δ 58.05 (s + Se satellites, $^1J_{PSe}$ = 894 Hz). EIMS, envelope centred on m/z 423.4 (M$^+$).

Crystallography

Diffraction-quality crystals of all compounds were obtained by slow evaporation of a solution of the appropriate compound: **I**, **1** and **4**; petrol: **2** and **3**; DCM: **5**; CDCl$_3$. Intensity data were collected on a Bruker X8 APEXII diffractometer using Mo-K$_\alpha$ X-radiation, with crystals mounted in inert oil on a cryoloop and cooled to 100 K by using an Oxford Cryosystems Cryostream. Indexing, data collection and absorption correction were performed using the APEXII suite of programs.[44] Using OLEX2,[45] structures were solved by direct methods using the SHELXS[46] or SHELXT[47] programme and refined by full-matrix least-squares (SHELXL).[46]

All crystals were single except those of **5** which was treated as a two-component twin. All crystals were also fully ordered and solvate-free, except those of compound **3**. In **3** the gold carboranylphosphine complex is fully ordered but there is a disordered solvent in the lattice that was impossible to satisfactorily model. Hence for this structure the intensity contribution of the disordered solvent was removed using the BYPASS procedure[48] implemented in OLEX2. The total electron count of the solvent per cell was 420e, which corresponds to 10 DCM molecules. These disordered solvent molecules predominantly occupy four voids of *ca.* 270 Å^3 each.

For all structures H atoms bound to cage B atoms were allowed to refine positionally whilst H atoms bound to C atoms were constrained to idealised geometries; C_{phenyl}–H = 0.95 Å, C_{methyl}–H = 0.98 Å, $C_{methylene}$–H = 0.99 Å. All H displacement parameters, U_{iso}, were constrained to be 1.2 × U_{eq} (bound B or C) except for Me H atoms [U_{iso}(H) = 1.5 × U_{eq} C(Me)]. Table 3 contains further experimental details.

Cone angle and percent buried volume calculations

Bis(carborane)phosphine cone angles were calculated from the crystallographically-determined structures using both the free

Table 3 Crystallographic data

	I	1	2	3·1.25CH₂Cl₂	4	5
CCDC	1527028	1527029	1527030	1527031	1527032	1527033
Formula	$C_{10}H_{25}B_{20}P$	$C_6H_{25}B_{20}P$	$C_{10}H_{25}AuB_{20}ClP$	$C_6H_{25}AuB_{20}ClP$	$C_{10}H_{25}B_{20}PSe$	$C_6H_{25}B_{20}PSe$
M	392.47	344.43	624.89	683.00	471.43	423.39
Crystal system	Triclinic	Monoclinic	Monoclinic	Orthorhombic	Monoclinic	Triclinic
Space group	$P\bar{1}$	$P2_1/n$	$C2/c$	$Pbca$	$P2_1/n$	$P\bar{1}$
$a/\text{Å}$	7.1139(10)	23.441(2)	17.0588(8)	10.4380(13)	10.3457(12)	7.1663(7)
$b/\text{Å}$	11.4378(14)	7.2690(6)	14.2499(7)	17.711(2)	16.9431(17)	11.0308(15)
$c/\text{Å}$	13.3912(15)	24.083(2)	20.0698(9)	27.475(3)	13.6941(14)	14.573(2)
$\alpha/°$	81.884(5)	90	90	90	90	111.478(9)
$\beta/°$	84.954(5)	108.290(5)	102.497(3)	90	105.612(6)	92.125(9)
$\gamma/°$	81.231(6)	90	90	90	90	104.679(6)
$U/\text{Å}^3$	1063.6(2)	3896.2(6)	4763.1(4)	5079.3(10)	2311.9(4)	1026.2(2)
Z, Z'	2, 1	8, 2	8, 1	8, 1	4, 1	2, 1
$F(000)/\text{e}$	400	1408	2368	2596	936	420
$D_{calc}/\text{Mg m}^{-3}$	1.225	1.174	1.743	1.786	1.354	1.370
$\mu(\text{Mo-K}_\alpha)/\text{mm}^{-1}$	0.127	0.128	6.357	6.224	1.693	1.898
$\theta_{max}/°$	26.46	23.77	32.01	27.24	28.95	30.14
Data measured	15 395	44 057	58 934	33 633	43 105	40 190
Unique data, n	4334	5928	8266	5651	6088	5691
R_{int}	0.0636	0.1415	0.0796	0.0526	0.0740	0.0763
R, wR_2 (obs. data)	0.0685, 0.1260	0.0795, 0.1841	0.0342, 0.0602	0.0297, 0.0585	0.0365, 0.0767	0.0410, 0.0861
S (all data)	1.135	1.053	1.015	1.020	1.034	1.036
Variables	340	609	358	323	349	315
$E_{max}, E_{min}/\text{e Å}^{-3}$	0.31, −0.35	0.48, −0.41	0.93, −1.81	0.69, −0.65	0.35, −0.42	0.61, −0.58

bis(carborane)phosphines (compounds **I** and **1**) and their AuCl complexes (compounds **2** and **3**), using the method of Müller and Mingos.[49] The P–M distance was set at 2.28 Å. %V_{bur} calculations were performed (again on all compounds **I**, **1–3**) using the Samb*V*ca software of Cavallo and co-workers,[50] with a sphere radius of 3.5 Å, a P–M distance of 2.28 Å and scaled Bondi radii.

Computational methods

All electronic structure calculations were carried out using the Gaussian 09 (Revision D.01)[51] program suite at the DFT level of theory. Geometries of all compounds were fully optimised without imposing symmetry constraints (C_1 symmetry), employing the BP86 functional.[52] Ahlrich's def2-TZVP basis of triple-ζ quality was used on P, Au, Cl, Se, and C and all hydrogen atoms of the ethyl group, while all B–H units of the carborane cage were described with the def2-SVP basis set.[53] The core electrons in Au were replaced by the Stuttgart–Dresden scalar relativistic effective core potential (SDD, ECP60MWB).[54] Optimised stationary points were characterised by analysis of their analytical second derivatives, with minima having only positive eigenvalues and transition states having exactly one imaginary eigenvalue. Subsequent geometry optimisations in both directions of the reaction coordinate were performed to confirm the minima linked by each transition state. The frequency calculations also provided thermal and entropic corrections to the total energy in the gas phase at T = 298.15 K and p = 1 atm within the rigid-rotor/harmonic oscillator (RRHO) approximation. Dispersion effects were accounted for by applying Grimme's van der Waals correction (D3 parameterization) protocol including

Becke–Johnson damping during the optimisations.[55] The topology of the electron density was analysed by means of QTAIM (quantum theory of atoms in molecules),[56] as implemented in the AIMAll package.[57] For **3-DFT**, inner shell electrons on Au modelled by the ECP were fitted by core density functions. Isotropic NMR spin–spin coupling constants were calculated using the coupled-perturbed SCF[58] method with the BHandHLYP[59] functional, which was found to yield the best agreement with experimental couplings. The *J*-couplings were obtained as the sum of all four Ramsey terms, *i.e.* Fermi contact (FC), spin–dipolar (SD), paramagnetic spin–orbit (PSO), and diamagnetic spin–orbit (DSO). The reported coupling constants have been averaged assuming free internal molecular rotation. The basis sets stated above were replaced by aug-cc-pVTZ-J[60] on P, and ethyl (C, H), as well as the cc-pVDZ[61] basis set (and the associated ECP for Au) on all other atoms. Effects due to the presence of a solvent were treated implicitly with a polarisable dielectric model, using the IEFPCM formalism in conjunction with Truhlar's SMD model.[62] The chosen dielectric constant (ε = 4.71) corresponds to that of chloroform. The compositions of molecular orbitals were analysed within the framework of localised natural bond orbitals, using the NBO 6.0 software.[63]

References

1 W. Y. Man, G. M. Rosair and A. J. Welch, *Acta Crystallogr., Sect. E: Struct. Rep. Online*, 2014, **70**, 462.

2 J. A. Dupont and M. F. Hawthorne, *J. Am. Chem. Soc.*, 1964, **86**, 1643.

3 S. Ren and Z. Xie, *Organometallics*, 2008, **27**, 5167.

4 D. Ellis, G. M. Rosair and A. J. Welch, *Chem. Commun.*, 2010, **46**, 7394.

5 D. Ellis, D. McKay, S. A. Macgregor, G. M. Rosair and A. J. Welch, *Angew. Chem., Int. Ed.*, 2010, **49**, 4943.

6 W. Y. Man, S. Zlatogorsky, H. Tricas, D. Ellis, G. M. Rosair and A. J. Welch, *Angew. Chem., Int. Ed.*, 2014, **53**, 12222.

7 M. J. Martin, W. Y. Man, G. M. Rosair and A. J. Welch, *J. Organomet. Chem.*, 2015, **798**, 36.

8 Z.-J. Yao, Y.-Y. Zhang and G.-X. Jin, *J. Organomet. Chem.*, 2015, **798**, 274.

9 D. Mandal, W. Y. Man, G. M. Rosair and A. J. Welch, *Acta Crystallogr., Sect. C: Cryst. Struct. Commun.*, 2015, **71**, 793.

10 G. Thiripuranathar, W. Y. Man, C. Palmero, A. P. Y. Chan, B. T. Leube, D. Ellis, D. McKay, S. A. Macgregor, L. Jourdan, G. M. Rosair and A. J. Welch, *Dalton Trans.*, 2015, **44**, 5628.

11 G. S. Kazakov, I. B. Sivaev, K. Yu. Suponitsky, D. D. Kirilin, V. I. Bregadze and A. J. Welch, *J. Organomet. Chem.*, 2016, **805**, 1.

12 D. Mandal, W. Y. Man, G. M. Rosair and A. J. Welch, *Dalton Trans.*, 2016, **45**, 15013.

13 L. E. Riley, A. P. Y. Chan, J. Taylor, W. Y. Man, D. Ellis, G. M. Rosair, A. J. Welch and I. B. Sivaev, *Dalton Trans.*, 2016, **45**, 1127.

14 W. Y. Man, D. Ellis, G. M. Rosair and A. J. Welch, *Angew. Chem., Int. Ed.*, 2016, **55**, 4596.

15 S. L. Powley, L. Schaefer, W. Y. Man, D. Ellis, G. M. Rosair and A. J. Welch, *Dalton Trans.*, 2016, **45**, 3635.

16 D. Zhao, J. Zhang, Z. Lin and Z. Xie, *Chem. Commun.*, 2016, **52**, 9992.

17 Y. O. Wong, M. D. Smith and D. V. Peryshkov, *Chem. – Eur. J.*, 2016, **22**, 6764.

18 Y. O. Wong, M. D. Smith and D. V. Peryshkov, *Chem. Commun.*, 2016, **52**, 12710.

19 K. O. Kirlikovali, J. C. Axtell, A. Gonzalez, A. C. Phung, S. I. Khan and A. M. Spokoyny, *Chem. Sci.*, 2016, **7**, 5132.

20 I. B. Sivaev, *Commun. Inorg. Synth.*, 2016, **4**, 21.

21 (*a*) D. A. Owen and M. F. Hawthorne, *J. Am. Chem. Soc.*, 1970, **92**, 3194; D. A. Owen and M. F. Hawthorne, *J. Am. Chem. Soc.*, 1971, **93**, 873; (*b*) R. A. Love and R. Bau, *J. Am. Chem. Soc.*, 1972, **94**, 8274; (*c*) D. E. Harwell, J. McMillan, C. B. Knobler and M. F. Hawthorne, *Inorg. Chem.*, 1997, **36**, 5951.

22 L. I. Zakharkin and N. F. Shemyakin, *Izv. Akad. Nauk SSSR, Ser. Khim.*, 1978, 1450.

23 A. I. Yanovsky, N. G. Furmanova, Yu. T. Struchkov, N. F. Shemyakin and L. I. Zakharkin, *Izv. Akad. Nauk SSSR, Ser. Khim.*, 1979, 1523.

24 S. E. Johnson and C. B. Knobler, *Phosphorus, Sulfur Silicon Relat. Elem.*, 1996, **115**, 227.

25 C. F. Macrae, I. J. Bruno, J. A. Chisholm, P. R. Edgington, P. McCabe, E. Pidcock, L. Rodriguez-Monge, R. Taylor, J. van de Streek and P. A. Wood, *J. Appl. Crystallogr.*, 2008, **41**, 466.

26 P. L. A. Popelier, *J. Phys. Chem. A*, 1998, **102**, 1873.

27 P. W. N. M. van Leeuwen, *Homogeneous Catalysis: Understanding the Art*, Kluwer, Dordrecht, The Netherlands, 2004.

28 Representative examples: (*a*) F. A. Hart and D. W. Owen, *Inorg. Chim. Acta*, 1985, **103**, L1; (*b*) C. Viñas, M. A. Flores, R. Núñez, F. Teixidor, R. Kivekäs and R. Sillanpää, *Organometallics*, 1998, **17**, 2278; (*c*) F. Teixidor, R. Núñez, M. A. Flores, A. Demonceau and C. Viñas, *J. Organomet. Chem.*, 2000, **614–615**, 48; (*d*) H.-S. Lee, J.-Y. Bae, J. Ko, Y. S. Kang, H. S. Kim, S.-J. Kim, J.-H. Chung and S. O. Kang, *J. Organomet. Chem.*, 2000, **614–615**, 83; (*e*) H.-S. Lee, J.-Y. Bae, J. Ko, Y. S. Kang, H. S. Kim and S. O. Kang, *Chem. Lett.*, 2000, **29**, 602; (*f*) H. Brunner, A. Apfelbacher and M. Zabel, *Eur. J. Inorg. Chem.*, 2001, 917; (*g*) H.-S. Lee, J.-Y. Bae, D.-H. Kim, H. S. Kim, S.-J. Kim, S. Cho, J. Ko and S. O. Kang, *Organometallics*, 2002, **21**, 210; (*h*) H. Wang, H.-S. Chan, J. Okuda and Z. Xie, *Organometallics*, 2005, **24**, 3118; (*i*) V. Lavallo, J. H. Wright, F. S. Tham and S. Quinlivan, *Angew. Chem., Int. Ed.*, 2013, **52**, 3172.

29 C. A. Tolman, *J. Am. Chem. Soc.*, 1970, **92**, 2956; C. A. Tolman, *Chem. Rev.*, 1977, **77**, 313.

30 A. C. Hillier, W. J. Sommer, B. S. Yong, J. L. Petersen, L. Cavallo and S. P. Nolan, *Organometallics*, 2003, **22**, 4322.

31 H. Clavier and S. P. Nolan, *Chem. Commun.*, 2010, **46**, 841.

32 (*a*) D. W. Allen and B. F. Taylor, *J. Chem. Soc., Dalton Trans.*, 1982, 51; (*b*) D. W. Allen, I. W. Nowell and B. F. Taylor, *J. Chem. Soc., Dalton Trans.*, 1985, 2505; (*c*) N. Anderson and B. Keay, *Chem. Rev.*, 2001, **101**, 997; (*d*) U. Beckmann, D. Süslüyan and P. C. Kunz, *Phosphorus, Sulfur Silicon Relat. Elem.*, 2011, **186**, 2061.

33 (*a*) C. J. Jameson and H. S. Gutowsky, *J. Chem. Phys.*, 1969, **51**, 2790; (*b*) C. J. Jameson, *J. Am. Chem. Soc.*, 1969, **91**, 6232; (*c*) W. McFarlane, *Proc. R. Soc. London, Ser. A*, 1968, **306**, 185.

34 (*a*) J. P. Alabrand, D. Gagnaire and J. B. Robert, *J. Mol. Spectrosc.*, 1968, **27**, 428; (*b*) A. R. Cullingworth, A. Pidcock and J. D. Smith, *Chem. Commun.*, 1966, 89.

35 Although the sign of $^1J_{\text{PSe}}$ has been determined to be negative (*e.g.* W. McFarlane and D. S. Rycroft, *J. Chem. Soc., Dalton Trans.*, 1973, 2162) it is conventionally reported as positive and we will follow this convention here.

36 A. R. Popescu, A. Laromaine, F. Teixidor, R. Sillanpää, R. Kivekäs, J. I. Llambias and C. Viñas, *Chem. – Eur. J.*, 2011, **17**, 4429.

37 P. Farràs, F. Teixidor, I. Rojo, R. Kivekäs, R. Sillanpää, P. González-Cardoso and C. Viñas, *J. Am. Chem. Soc.*, 2011, **133**, 16537.

38 A. Muller, S. Otto and A. Roodt, *Dalton Trans.*, 2008, 650.

39 J. A. Davies, S. Dutremez and A. A. Pinkerton, *Inorg. Chem.*, 1991, **30**, 2380.

40 S. Otto, A. Ionescu and A. Roodt, *J. Organomet. Chem.*, 2005, **690**, 4337.

41 C. R. Groom and F. H. Allen, *Angew. Chem., Int. Ed.*, 2014, **53**, 662. For this search we used ConQuest and version 5.37 of the CSD (November 2015).

42 (*a*) SUNKIX, P=Se 2.073(9), 2.079(3) Å: Y. Sun, M.-Q. Yan, Y. Liu, Z.-Y. Lian, T. Meng, S.-H. Liu, J. Chen and G.-A. Yu, *RSC Adv.*, 2015, **5**, 71437; (*b*) BAZWEF, P=Se 2.073(3) Å: T. Stampfl, R. Gutmann, G. Czermak, C. Langes, A. Dumfort, H. Kopacka, K.-H. Ongania and P. Bruggeller, *Dalton Trans.*, 2003, 3425; (*c*) DAHROV, P=Se 2.0588(9), 2.0770(9) Å: K. D. Reichl, C. L. Mandell, O. D. Henn, W. G. Dougherty, W. S. Kassel and C. Nataro, *J. Organomet. Chem.*, 2011, **696**, 3882; (*d*) NIKBIS, P=Se 2.075(15) Å: Q. Zhang, M. Hong and H. Liu, *Transition Met. Chem.*, 1997, **22**, 156; (*e*) PPHSEA, P=Se 2.0697(17) Å: O. Orama, K. Nieminen, M. Karhu and R. Uggla, *Cryst. Struct. Commun.*, 1979, **8**, 909; (*f*) UXIWUU, P=Se 2.079(3) Å: R. Kabe, V. M. Lynch and P. Anzenbacher Jr., *CrystEngComm*, 2011, **13**, 5423; (*g*) VUHJIR, P=Se 2.055(3), 2.056(4), 2.065(3) Å: M. Birkel, J. Schulz, U. Bergstrasser and M. Regitz, *Angew. Chem., Int. Ed.*, 1992, **31**, 879.

43 R. Uson, A. Laguna and M. Laguna, *Inorg. Synth.*, 1989, **26**, 85.

44 *Bruker AXS APEX2, version 2009-5*, Bruker AXS Inc., Madison, Wisconsin, USA, 2009.

45 O. V. Dolomanov, L. J. Bourhis, R. J. Gildea, J. A. K. Howard and H. Puschmann, *J. Appl. Crystallogr.*, 2009, **42**, 339.

46 G. M. Sheldrick, *Acta Crystallogr., Sect. A: Fundam. Crystallogr.*, 2008, **64**, 112.

47 G. M. Sheldrick, *Acta Crystallogr., Sect. A: Fundam. Crystallogr.*, 2015, **71**, 3.

48 (*a*) P. van der Sluis and A. L. Spek, *Acta Crystallogr., Sect. A: Fundam. Crystallogr.*, 1990, **46**, 194; (*b*) A. L. Spek, *J. Appl. Crystallogr.*, 2003, **36**, 7.

49 (*a*) T. E. Müller and D. M. P. Mingos, *Transition Met. Chem.*, 1995, **20**, 533; (*b*) D. M. P. Mingos in *Modern Coordination Chemistry: The Legacy of Joseph Chatt*, RSC, Cambridge, 2002, p. 69.

50 (*a*) A. Poater, B. Cosenza, A. Correa, S. Giudice, F. Ragone, V. Scarano and L. Cavallo, *Eur. J. Inorg. Chem.*, 2009, **2009**, 1759; (*b*) http://www.molnac.unisa.it/OMtools/sambvca.php.

51 M. J. Frisch, G. W. Trucks, H. B. Schlegel, G. E. Scuseria, M. A. Robb, J. R. Cheeseman, G. Scalmani, V. Barone, B. Mennucci, G. A. Petersson, H. Nakatsuji, M. Caricato, X. Li, H. P. Hratchian, A. F. Izmaylov, J. Bloino, G. Zheng, J. L. Sonnenberg, M. Hada, M. Ehara, K. Toyota, R. Fukuda, J. Hasegawa, M. Ishida, T. Nakajima, Y. Honda, O. Kitao, H. Nakai, T. Vreven, J. A. Montgomery Jr., J. E. Peralta, F. Ogliaro, M. Bearpark, J. J. Heyd, E. Brothers, K. N. Kudin, V. N. Staroverov, T. Keith, R. Kobayashi, J. Normand, K. Raghavachari, A. Rendell, J. C. Burant, S. S. Iyengar, J. Tomasi, M. Cossi, N. Rega, J. M. Millam, M. Klene, J. E. Knox, J. B. Cross, V. Bakken, C. Adamo, J. Jaramillo, R. Gomperts, R. E. Stratmann, O. Yazyev, A. J. Austin, R. Cammi, C. Pomelli, J. W. Ochterski, R. L. Martin, K. Morokuma, V. G. Zakrzewski, G. A. Voth, P. Salvador, J. J. Dannenberg, S. Dapprich, A. D. Daniels, O. Farkas, J. B. Foresman, J. V. Ortiz, J. Cioslowski and D. J. Fox, *Gaussian 09, Revision D.01*, Gaussian, Inc., Wallingford, CT, 2013.

52 (*a*) A. D. Becke, *Phys. Rev. A*, 1988, **38**, 3098; (*b*) J. P. Perdew, *Phys. Rev. B: Condens. Matter*, 1986, **33**, 8822.

53 F. Weigend and R. Ahlrichs, *Phys. Chem. Chem. Phys.*, 2005, **7**, 3297.

54 D. Andrae, U. Haussermann, M. Dolg, H. Stoll and H. Preuss, *Theor. Chim. Acta*, 1990, **77**, 123.

55 (*a*) S. Grimme, J. Antony, S. Ehrlich and H. Krieg, *J. Chem. Phys.*, 2010, **132**, 154104; (*b*) A. D. Becke and E. R. Johnson, *J. Chem. Phys.*, 2005, **122**, 154101; (*c*) S. Grimme, S. Ehrlich and L. Goerigk, *J. Comput. Chem.*, 2011, **32**, 1456.

56 R. F. W. Bader, *Atoms in Molecules: A Quantum Theory*, Oxford University Press, 1990.

57 T. A. Keith, *AIMAll (Version 13.02.26)*, TK Gristmill Software, Overland Park KS, USA, 2014 (aim.tkgristmill.com), 1997–2013.

58 (*a*) V. Sychrovský, J. Gräfenstein and D. Cremer, *J. Chem. Phys.*, 2000, **113**, 3530; (*b*) T. Helgaker, M. Watson and N. C. Handy, *J. Chem. Phys.*, 2000, **113**, 9402; (*c*) V. Barone, J. E. Peralta, R. H. Contreras and J. P. Snyder, *J. Phys. Chem. A*, 2002, **106**, 5607.

59 (*a*) A. D. Becke, *J. Chem. Phys.*, 1993, **98**, 5648; (*b*) C. Lee, W. Yang and R. G. Parr, *Phys. Rev. B: Condens. Matter*, 1988, **37**, 785; (*c*) B. Miehlich, A. Savin, H. Stoll and H. Preuss, *Chem. Phys. Lett.*, 1989, **157**, 200; (*d*) A. D. Becke, *J. Chem. Phys.*, 1993, **98**, 1372.

60 (*a*) P. F. Provasi, G. A. Aucar and S. P. A. Sauer, *J. Chem. Phys.*, 2001, **115**, 1324; (*b*) J. E. Peralta, G. E. Scuseria, J. R. Cheeseman and M. J. Frisch, *Chem. Phys. Lett.*, 2003, **375**, 452.

61 (*a*) T. H. Dunning Jr., *J. Chem. Phys.*, 1989, **90**, 1007; (*b*) A. K. Wilson, D. E. Woon, K. A. Peterson and T. H. Dunning Jr., *J. Chem. Phys.*, 1999, **110**, 7667; (*c*) K. A. Peterson and C. Puzzarini, *Theor. Chem. Acc.*, 2005, **114**, 283.

62 A. V. Marenich, C. J. Cramer and D. G. Truhlar, *J. Phys. Chem. B*, 2009, **113**, 6378.

63 E. D. Glendening, J. K. Badenhoop, A. E. Reed, J. E. Carpenter, J. A. Bohmann, C. M. Morales, C. R. Landis and F. Weinhold, *NBO 6.0*, Theoretical Chemistry Institute, University of Wisconsin, Madison, WI, 2013; http://nbo6.chem.wisc.edu/.